Journal of Sound and Vibration (1999) **222**(4), 531–546
Article No. jsvi.1999.2119, available online at http://www.idealibrary.com on IDEAL

SPACE-HARMONIC ANALYSIS OF INPUT POWER FLOW IN A PERIODICALLY STIFFENED SHELL FILLED WITH FLUID

M. B. XU, X. M. ZHANG AND W. H. ZHANG
Department of Naval Architecture and Ocean Engineering, Huazhong University of Science and Technology, 430074 *Wuhan, Hubei, People's Republic of China*

(*Received* 12 *May* 1998, *and in final form* 19 *October* 1998)

In this paper, the input power flow from a cosine harmonic circumferential line force into an infinite cylindrical fluid-filled shell with periodic stiffeners is studied. The stiffeners are idealized as line attachments capable of exerting line forces which relate to the stiffeners and the shell. The motion of the shell and the pressure field in the contained fluid are described by the Flügge thin shell theory and the Helmholt equation respectively. A periodic structure theory, space-harmonic analysis, is used to investigate this fluid-filled periodic structure. The concept of the vibrational power flow is introduced and the influence of the parameters of the stiffeners upon the results is also dscussed.

1. INTRODUCTION

Many engineering structures, such as multi-span bridges, stiffened plates and the shells in aerospace and ship structure, pipelines, can be treated as periodic structures. The vibration of these periodic structures has been investigated by using various methods, such as receptance methods, transfer matrices, direct solutions, space-harmonic analysis, energy method and the method of phased arrays of forces and moments.

Since the stiffened cylindrical shells, an important kind of periodic structures, are widely used in many industrial and defense fields, the dynamic response of periodic shells is an important topic and has been analyzed by several authors. Lin and McDaniel [1] used the transfer matrix method to study both the free and forced vibrations of a periodic shell. Using direct solutions, Mead and Bardell [2, 3] studied the free wave motion in a thin cylindrical shell with periodic stiffening either around the circumference or along the length. The propagation constant curves were obtained for a particular circumferential stiffened shell. Zhang and Zhang [4] combined the theory of periodic structures and the power flow analysis, and discussed the power flow input and transmitted along the shell.

As the periodic shell is filled with fluid, due to the influence of the contained fluid, the number of the coupling co-ordinates between adjacent periodic element

0022–460X/99/190531 + 16 $30.00/0

will be infinite. Then the above mentioned methods are no longer suitable and an alternative method has to be employed to study this fluid coupled periodic structure system. The studies by Mead [5] demonstrated that the flexural wave in a periodic beam must be regarded as a wave group. Accordingly the response to a converted harmonic pressure can be regarded as an infinite sum of space harmonics and the effects of fluid loading on the forced harmonic response can easily be included by using space-harmonic analysis.

The method of space harmonics was adopted by Mead and Pujara [6] to investigate the response of periodically supported beams due to a spatial and temporal harmonic pressure in the form of a particular series of space harmonic. Mace [7] considered the vibration of and sound radiation from a two-dimensional fluid-loaded plate periodically stiffened in one direction and excited by a convected pressure field of plane harmonic waves. Mace [8] proceeded to discuss the same periodic plate excited either by a line force parallel to the stiffeners or by a point force at an arbitrary location.

The concept of vibrational power flow is very valuable in the analysis of noise and vibration of a shell. Without considering the influence of stiffeners, Fuller [9] investigated the forced input mobility of an infinite elastic circular cylindrical shell filled with fluid. The spectral equations of motion of the shell–fluid system and the method of residues are employed to evaluate the mobility, and their physical interpretation is also discussed. Zhang and Zhang [4] introduced the concept of power flow into the analyss of periodic shells, studied the input vibrational power flow from a cosine harmonic circumferential line force and the power transmitted by internal forces of the shell wall. But the influence of the fluid was not considered in their research.

In the analysis in this paper, both the influence of the stiffeners and that of the contained fluid upon the elastic cylindrical shell are considered. Space-harmonic analysis is adopted to investigate the dynamic response of an infinite fluid-filled shell with periodic circumferential stiffeners. The simple harmonic motion of the shell and the pressure field in the fluid are described by Flügge's dynamic shell equations and Helmholtz's equation respectively. Firstly, the response of the structure to a convected harmonic pressure is given. Then, the response to a cosine harmonic circumferential line force is investigated. Moreover, the input vibrational power flow into the structure is given and the influence of the stiffeners' parameters on the results is also discussed.

2. RESPONSE OF A PERIODICALLY STIFFENED SHELL TO CONVECTED HARMONIC PRESSURE

An infinite cylindrical thin-walled fluid-filled shell reinforced with equally spaced ring stiffeners shown in Figure 1 is considered. Let R and h be the mean radius and thickness of the shell. Let E, μ and ρ be the Young's modulus, the Possion's ratio and the density of the shell material. The density of the contained fluid is ρ_0 and the sound velocity in it is c_0. The ring stiffeners have uniform rectangular section with width b and height d, attached at $x = mL$ (L is the stiffener spacing, $m = 0, \pm 1, \pm 2 \cdots$). The connections are rigid, so that, at each

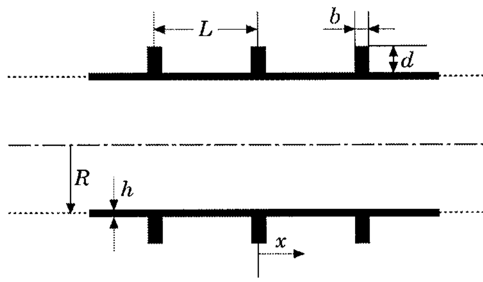

Figure 1. Periodically stiffened shell filled-with fluid.

line of attachment, the shell and stiffener have the same linear velocity and angular velocity. The stiffeners may exert axial force, shear, and moments on the shell. To simplify the problem, it is assumed that the stiffeners are located on the outer wall of the shell, so that their interaction with the contained fluid (air) can be ignored.

2.1. EQUATIONS OF MOTION OF THE PERIODIC SHELL

The shell is excited by a harmonic pressure p, expressed as

$$p(x, \theta, t) = p = p_0 \exp(\mathrm{i}\omega t - \mathrm{i}k_x x) \cos(n\theta) \tag{1}$$

where ω is the circular frequency, k_x is the axial wavenumber and n is the circumferential modal number.

For the sake of brevity, let the term $e^{\mathrm{i}\omega t}$ be excluded from now on. The cylindrical co-ordinate system (x, θ, r) is adopted in the analysis. The simultaneous vibrations of the shell are described by Flügge's shell equations [9]

$$L_1(u, v, w) = f_u, \qquad L_2(u, v, w) = f_v, \qquad L_3(u, v, w) = f_w. \tag{2}$$

where u, v, and w are the displacements of the shell in the direction of the x-, θ- and r-axes respectively. L_i denote linear different operators which are not given here for the sake of brevity. f_u, f_v and f_w are the external loads exerted on the shell wall in the direction of the x-, θ- and r-axes respectively, which are given by the equations

$$f_u = D \sum_{-\infty}^{\infty} F_{u,m} \delta(x - mL), \qquad f_v = D \sum_{-\infty}^{\infty} F_{v,m} \delta(x - mL), \tag{3a, b}$$

$$f_w = D \left\{ p - p_f + \sum_{m=-\infty}^{\infty} F_{w,m} \delta(x - mL) + \sum_{m=-\infty}^{\infty} M_m \delta'(x - mL) \right\}, \tag{3c}$$

$$D = R^2(1 - \mu^2)/(Eh), \tag{4}$$

where p is the applied pressure load, p_f is the "acoustic" pressure exerted by the contained fluid, $F_{u,m}$, $F_{v,m}$, $F_{w,m}$ and M_m are the sideward forces or moments of the mth stiffener acting on the shell and δ is the Dirac delta function.

The pressure field in the contained fluid satisfies the acoustic wave equation in cylindrical co-ordinates,

$$\Delta p_f + k_0^2 p_f = 0, \tag{5}$$

where k_0 is the free wave number in the contained fluid and $k_0 = \omega/c_0$.

To ensure that the fluid remains in contact with the shell wall, the fluid radial displacement and the shell radial displacement must be equal at the interface of the shell inner wall and the fluid. The coupling condition is then $w_{fluid} = w_{shell}$ at $r = R$.

Taking the Fourier transform of equations (2) and (5) and applying the coupling condition, the following equations are obtained:

$$[\mathbf{L}_{3\times 3}]\begin{Bmatrix} \tilde{U} \\ \tilde{V} \\ \tilde{W} \end{Bmatrix} = \begin{Bmatrix} \tilde{F}_{u,shell} \\ \tilde{F}_{v,shell} \\ \tilde{F}_{load} + \tilde{F}_{w,shell} + \tilde{M}_{shell} \end{Bmatrix}, \tag{6}$$

where, $\tilde{U}$, $\tilde{V}$ and $\tilde{W}$ are the spectral displacements, matrix $\mathbf{L}$ is symmetric,

$$[\mathbf{L}_{3\times 3}] = \begin{bmatrix} \lambda^2 + a' & b'\lambda & c'\lambda^3 + d'\lambda \\ & e'\lambda^2 + f' & g'\lambda^2 + h' \\ & & j' + k'\lambda^2 + l'\lambda^4 - FL \end{bmatrix} \tag{7}$$

$$\tilde{F}_{load} = \int_{-\infty}^{\infty} Dp_0\, \mathrm{e}^{\mathrm{i}kx}\, \mathrm{e}^{-\mathrm{i}k_x x}\, \mathrm{d}x = Dp_0 \delta(k - k_x), \tag{8}$$

$$\tilde{F}_{u,shell} = D\int_{-\infty}^{\infty} \sum_{m=-\infty}^{\infty} F_{u,m}\delta(x - mL)\, \mathrm{e}^{\mathrm{i}kx}\, \mathrm{d}x = D\sum_{m=-\infty}^{\infty} F_{u,m}\, \mathrm{e}^{\mathrm{i}kmL}, \tag{9a}$$

$$\tilde{F}_{v,shell} = D\int_{-\infty}^{\infty} \sum_{m=-\infty}^{\infty} F_{v,m}\delta(x - mL)\, \mathrm{e}^{\mathrm{i}kx}\, \mathrm{d}x = D\sum_{m=-\infty}^{\infty} F_{v,m}\, \mathrm{e}^{\mathrm{i}kmL}, \tag{9b}$$

$$\tilde{F}_{w,shell} = D\int_{-\infty}^{\infty} \sum_{m=-\infty}^{\infty} F_{w,m}\delta(x - mL)\, \mathrm{e}^{\mathrm{i}kx}\, \mathrm{d}x = D\sum_{m=-\infty}^{\infty} F_{w,m}\, \mathrm{e}^{\mathrm{i}kmL}, \tag{9c}$$

$$\tilde{M}_{shell} = D\int_{-\infty}^{\infty} \sum_{m=-\infty}^{\infty} M_m\delta'(x - mL)\, \mathrm{e}^{\mathrm{i}kx}\, \mathrm{d}x = -\mathrm{i}Dk_x\sum_{m=-\infty}^{\infty} M_m\, \mathrm{e}^{\mathrm{i}kmL}. \tag{9d}$$

In equation (7),

$$\lambda = k_x R, \qquad a' = -(1-\mu)(1+k)n^2/2 + \Omega^2, \qquad b' = (1+\mu)n/2, \quad c' = -k, \tag{10a–d}$$

$$d' = \mu - k(1-\mu)n^2/2, \qquad e' = -(1-\mu)(1+3k)/2, \qquad f' = n^2 - \Omega^2, \tag{10e–g}$$

$$g' = -(3-\mu)kn/2, \quad h' = n, \quad j' = 1 + k(n^2-1)^2 - \Omega^2, \quad k' = -2n^2k, \quad \text{(10h–k)}$$

$$l' = k, \qquad \Omega^2 = \rho R^2\omega^2(1-\mu^2)/E, \qquad k = h^2/12R^2, \qquad \text{(10l–n)}$$

where Ω is the non-dimensional frequency, FL is the fluid loading term due to the coupling between the structure and the fluid, expressed as follows [9],

$$FL = \Omega^2(\rho_0/\rho)(R/h)(\mathrm{J_n}(\mathrm{k_s^r R})/(\mathrm{k_s^r R})\mathrm{J_n}(\mathrm{k_s^r R}), \qquad (11)$$

where $\mathrm{J}_n()$ is a Bessel function of order n, $k_s^r = \pm\sqrt{(k_0)^2 - (k_x)^2}$ is the radial fluid wavenumber and a prime denotes differention with respect to the argument $k_s^r R$.

In equations (9), the forces in the stiffeners acting on the outer shell wall satisfy the periodicity relation since the structure is periodic. Then,

$$\begin{Bmatrix} F_{u,m} \\ F_{v,m} \\ F_{w,m} \\ M_m \end{Bmatrix} = \mathrm{e}^{-\mathrm{i}mk_xL} \begin{Bmatrix} F_{u,0} \\ F_{v,0} \\ F_{w,0} \\ M_0 \end{Bmatrix}. \qquad (12)$$

By using the Poisson sum formula [7],

$$\sum_{m=-\infty}^{\infty} \mathrm{e}^{-\mathrm{i}k_x mL}\,\mathrm{e}^{\mathrm{i}kmL} = 2\pi \sum_{m=-\infty}^{\infty} \delta[2m\pi + (k_x - k)L] \qquad (13)$$

The following equations can be obtained

$$\tilde{F}_{u,shell} = 2\pi D F_{u,0} \sum_{m=-\infty}^{\infty} \delta[2m\pi + (k_x - k)L], \qquad (14a)$$

$$\tilde{F}_{v,shell} = 2\pi D F_{v,0} \sum_{m=-\infty}^{\infty} \delta[2m\pi + (k_x - k)L], \qquad (14b)$$

$$\tilde{F}_{w,shell} = 2\pi D F_{w,0} \sum_{m=-\infty}^{\infty} \delta[2m\pi + (k_x - k)L], \qquad (14c)$$

$$\tilde{M}_{shell} = -\mathrm{i}\pi D k_x M_0 \sum_{m=-\infty}^{\infty} \delta[2m\pi + (k_x - k)L]. \qquad (14d)$$

Let matrix $\mathbf{I}$ be the inverse of matrix $\mathbf{L}$ (equation (7)), then the spectral displacements can be obtained from equation (6) as follows:

$$\begin{Bmatrix} \tilde{U} \\ \tilde{V} \\ \tilde{W} \end{Bmatrix} = \begin{bmatrix} I_{11} & I_{12} & I_{13} \\ & I_{22} & I_{23} \\ & & I_{33} \end{bmatrix} \begin{Bmatrix} \tilde{F}_{u,shell} \\ \tilde{F}_{v\,shell} \\ \tilde{F}_{load} + \tilde{F}_{w,shell} + \tilde{M}_{shell} \end{Bmatrix}, \qquad (15)$$

where, I_{11}, I_{12}, I_{13}, I_{22}, I_{23} and I_{33} can be written in terms of the elements of matrix **L** from matrix theory.

Taking the inverse transform of equations (15), the shell displacements are obtained as

$$\begin{aligned}\frac{u(x)}{D} = {} & \frac{P_0}{2\pi} I_{13}(k_x)\exp(-\mathrm{i}k_x x) + F_{u,0}\sum_{m=-\infty}^{\infty}[\exp(-\mathrm{i}k_m x)I_{11}(k_m)] \\ & + F_{v,0}\sum_{m=-\infty}^{\infty}[\exp(-\mathrm{i}k_m x)I_{12}(k_m)] + F_{w,0}\sum_{m=-\infty}^{\infty}[\exp(-\mathrm{i}k_m x)I_{13}(k_m)] \\ & - \mathrm{i}M_0\sum_{m=-\infty}^{\infty}[\exp(-\mathrm{i}k_m x)k_m I_{13}(k_m)], \end{aligned} \tag{16a}$$

$$\begin{aligned}\frac{v(x)}{D} = {} & \frac{P_0}{2\pi} I_{23}(k_x)\exp(-\mathrm{i}k_x x) + F_{u,0}\sum_{m=-\infty}^{\infty}[\exp(-\mathrm{i}k_m x)I_{12}(k_m)] \\ & + F_{v,0}\sum_{m=-\infty}^{\infty}[\exp(-\mathrm{i}k_m x)I_{22}(k_m)] + F_{w,0}\sum_{m=-\infty}^{\infty}[\exp(-\mathrm{i}k_m x)I_{23}(k_m)] \\ & - \mathrm{i}M_0\sum_{m=-\infty}^{\infty}[\exp(-\mathrm{i}k_m x)k_m I_{23}(k_m)], \end{aligned} \tag{16b}$$

$$\begin{aligned}\frac{w(x)}{D} = {} & \frac{P_0}{2\pi} I_{33}(k_x)\exp(-\mathrm{i}k_x x) + F_{u,0}\sum_{m=-\infty}^{\infty}[\exp(-\mathrm{i}k_m x)I_{13}(k_m)] \\ & + F_{v,0}\sum_{m=-\infty}^{\infty}[\exp(-\mathrm{i}k_m x)I_{23}(k_m)] + F_{w,0}\sum_{m=-\infty}^{\infty}[\exp(-\mathrm{i}k_m x)I_{33}(k_m)] \\ & - \mathrm{i}M_0\sum_{m=-\infty}^{\infty}[\exp(-\mathrm{i}k_m x)k_m I_{33}(k_m)], \end{aligned} \tag{16c}$$

Then, the displacements at $x = 0$ are given as

$$\begin{aligned}\frac{1}{D}u(0) = {} & \frac{1}{2\pi}p_0 I_{13}(k_x) + F_{u,0}\sum_{m=-\infty}^{\infty} I_{11}(k_m) + F_{v,0}\sum_{m=-\infty}^{\infty} I_{12}(k_m) \\ & + F_{w,0}\sum_{m=-\infty}^{\infty} I_{13}(k_m) - \mathrm{i}M_0\sum_{m=-\infty}^{\infty}[k_m I_{13}(k_m)], \end{aligned} \tag{17a}$$

$$\frac{1}{D}v(0) = \frac{1}{2\pi}p_0 I_{23}(k_x) + F_{u,0}\sum_{m=-\infty}^{\infty} I_{12}(k_m) + F_{v,0}\sum_{m=-\infty}^{\infty} I_{22}(k_m)$$
$$+ F_{w,0}\sum_{m=-\infty}^{\infty} I_{23}(k_m) - \mathrm{i}M_0\sum_{m=-\infty}^{\infty} [k_m I_{23}(k_m)], \tag{17b}$$

$$\frac{1}{D}w(0) = \frac{1}{2\pi}p_0 I_{33}(k_x) + F_{u,0}\sum_{m=-\infty}^{\infty} I_{13}(k_m) + F_{v,0}\sum_{m=-\infty}^{\infty} I_{23}(k_m)$$
$$+ F_{w,0}\sum_{m=-\infty}^{\infty} I_{33}(k_m) - \mathrm{i}M_0\sum_{m=-\infty}^{\infty} [k_m I_{33}(k_m)], \tag{17c}$$

where

$$k_m = k_x + 2m\pi/L. \tag{18}$$

2.2. BOUNDARY CONDITIONS BETWEEN THE SHELL AND THE STIFFENERS

Once the forces and moments of the 0th stiffener in equation (17) are given, the shell response to the applied pressure load $p(x, \theta, t)$ can be solved. Expressions for the reaction forces and moments of the stiffeners can be obtained by equating the displacements and the slopes of the shell and the ring stiffener.

The reaction forces in the line circumferential stiffener at $x = 0$ can be expressed as follows:

$$F_{w,0} = -K_1 w(0) - K_2 v(0), \qquad F_{v,0} - K_2 w(0) + K_3 v(0) \tag{19a, b}$$

$$F_{u,0} = K_4 u(0) + \left(K_5 - \frac{e_1}{R}K_4\right)\left(R\frac{\partial w}{\partial x}(0)\right) = K_4 u(0) + \left(K_5 - \frac{e_1}{R}K_4\right)(-\mathrm{i}k_x R w(0)), \tag{19c}$$

$$M_0 = K_5 u(0) + \left(K_6 - \frac{e_1}{R}K_5\right)\left(R\frac{\partial w}{\partial x}(0)\right) = K_5 u(0) + \left(K_6 - \frac{e_1}{R}K_5\right)(-\mathrm{i}k_x R w(0)), \tag{19d}$$

where e_1 is the distance from the midsurface of the shell to the geometric center of stiffener. K_1, K_2, K_3, K_4, K_5 and K_6 are given in the Appendix A.

2.3. SOLUTION OF THE SHELL RESPONSE

Introducing equations (19) into (17), the shell displacement at $x = 0$ can be obtained in matrix form as:

$$\mathbf{K}\begin{bmatrix} u(0) \\ v(0) \\ w(0) \end{bmatrix} = \begin{bmatrix} K_{11} & K_{12} & K_{13} \\ K_{21} & K_{22} & K_{23} \\ K_{31} & K_{32} & K_{33} \end{bmatrix}\begin{bmatrix} u(0) \\ v(0) \\ w(0) \end{bmatrix} = \begin{bmatrix} F^u \\ F^v \\ F^w \end{bmatrix} \tag{20}$$

where the elements of matrix **K** can be easily obtained and thus not given here for the sake of brevity, and where

$$F^u = \frac{1}{2\pi} p_0 I_{13}(k_x), \qquad F^v = \frac{1}{2\pi} p_0 I_{23}(k_x), \qquad F^w = \frac{1}{2\pi} p_0 I_{33}(k_x). \tag{21a–c}$$

Let matrix **Q** be the inverse of matrix **K**, then the displacements of the stiffened shell at $x = 0$ can be obtained as follows

$$\begin{bmatrix} u(0) \\ v(0) \\ w(0) \end{bmatrix} = \begin{bmatrix} Q_{11} & Q_{12} & Q_{13} \\ Q_{21} & Q_{22} & Q_{23} \\ Q_{31} & Q_{32} & Q_{33} \end{bmatrix}\begin{bmatrix} F^u \\ F^v \\ F^w \end{bmatrix} \tag{22}$$

where the elements of matrix **Q** can be written in terms of the element of matrix **K** from matrix theory and not given for shortness.

Once the displacements of the stiffened shell at $x = 0$ are given, the reaction forces and moments of the 0th stiffener can be obtained from equations (19), and thus the displacements of the stiffened shell $u(x)$, $v(x)$ and $w(x)$ can be obtained from equations (16). The expressions are very complex and thus not given here.

3. RESPONSE OF THIS PERIODIC SHELL TO A COSINE HARMONIC CIRCUMFERENTIAL LINE FORCE

Any time–harmonic excitation can be decomposed into convected harmonic pressure by taking the Fourier transform.

According to the theory of Fourier transform,

$$\delta(x) = \frac{1}{2\pi}\int_{-\infty}^{\infty} \mathrm{e}^{-\mathrm{i}kx}\, \mathrm{d}x \tag{23}$$

For a cosine harmonic circumferential line force $F = p_0\delta(x)\mathrm{e}^{\mathrm{i}\omega t}\cos(n\theta)$, it can be written as the form of convected pressure where $p = p_0\,\mathrm{e}^{\mathrm{i}\omega t - ik_x x}\cos(n\theta)$ as

$$F = \frac{1}{2\pi}\int_{-\infty}^{\infty} p\, \mathrm{d}k_x. \tag{24}$$

Then, from equation (22), the response at $x = 0$ of this periodic structure to a cosine harmonic circumferential line force can be expressed as

$$w(0) = \frac{1}{2\pi}\int_{-\infty}^{\infty} (Q_{31}F^u + Q_{32}F^v + Q_{33}F^w)\mathrm{d}k_x. \tag{25}$$

The response of this system at any other position $w(x)$ can also be obtained and the response to any other exciting force can also be obtained in the same manner.

In order to obtain the shell response, the intergal in equation (25) must be evaluated. In equation (25), the elements of matrix **Q** can be written in terms of the element of matrix **K** in equation (20), and the element of matrix **K** can be in terms of the infinite sums

$$\sum_{m=-\infty}^{\infty} I_{11}(k_m), \qquad \sum_{m=-\infty}^{\infty} I_{12}(k_m), \ldots, \sum_{m=-\infty}^{\infty} I_{33}(k_m)$$

and

$$\sum_{m=-\infty}^{\infty} [k_m I_{13}(k_m)], \qquad \sum_{m=-\infty}^{\infty} [k_m I_{23}(k_m)], \qquad \sum_{m=-\infty}^{\infty} [k_m I_{33}(k_m)]$$

in equation (17).

In [7] Mace has pointed out that, when fluid loading is neglected, the infinite sums for a stiffened plate (similar to the infinite sums for a stiffened shell in equation (17)) can be evaluated by using the Poisson sum formula, but the derivation is very complex and intricate. These infinite sums can also be obtained by using the numerical method and results show good agreement between the numerical values and the accurate values. When the effects of the fluid loading is considered, these infinite sums cannot be evaluated explicitly and must be evaluated aproximately by using the numerical method.

Once these infinite sums in equation (17) are obtained, the elements of matrix **Q** in equation (25) can be calculated easily and thus the intergal in equation (25) can be evaluated.

A integral for a stiffened plate (similar to the integral for a stiffened shell) has been discussed by Mace [8]. When fluid loading is neglected, the integral can be evaluated by contour integration. When the effects of fluid loading are included, the integral cannot be evaluated explicitly and it is probably easiest to deal with it by numerical integration. In this article an integrated numerical method discussed in reference [10] is employed to calculate the intergral. This method is to integrate numerically along the pure imaginary axis of the complex wavenumber domain. Some damping is introduced into the shell material in order to avoid singularities in the integrand function along the integration path. Damping is introduced into the shell material by modifying the Young's modules E to be complex such that $E' = E(1 - i\eta)$. The solution of free wavenumbers of this system is unnecessary and the method is simple. Moreover, this method is found to provide sufficient accuracy and the value of loss factor η has an insignificant effect on the final results.

4. POWER FLOW ANALYSIS

When a harmonic force $F = F_0\,e^{i\omega t}$ is applied radially to a point of the shell wall, a radial velocity $\partial w/\partial t = \dot{w} = \dot{w}_0\,e^{i\omega t+\varphi}$ is generated at the same point. The input vibrational power flow from this point is defined as in reference [10]

$$P_{point} = \frac{1}{T}\int_0^T F\dot{w}\,\mathrm{d}t = \tfrac{1}{2}F_0\dot{w}_0\cos\varphi = \tfrac{1}{2}\mathrm{Re}\{F_0(\dot{w})^{\otimes}\}, \tag{26}$$

where φ is the phase difference and $^{\otimes}$ denotes the complex conjugate.

Then the total input power flow for a line harmonic force applied in the radial direction of the shell is obtained as follows:

$$P_{line} = \int_0^{2\pi} P_{point} R\,\mathrm{d}\theta = \eta_n \pi\ \mathrm{Re}\{\mathrm{i}\omega(F_0 w)^{\otimes}\}, \tag{27}$$

where $\eta_{n=0} = 1$ and $\eta_{n>0} = 0{\cdot}5$.

The non-dimensional power flow is defined as:

$$P'_{line} = P_{line}\sqrt{\rho E R^2(1-\mu^2)}/(F_0^2\pi). \tag{28}$$

5. RESULTS AND DISCUSSION

In order to make sure that the derivation and analysis are correct, an unstiffened cylindrical fluid-filled shell is investigated both by this method and by the method discussed in reference [9]. The input power flow is shown in Figure 2. It shows that the results obtained by this method is almost the same as those produced in reference [9]. Hence a conclusion can be drawn that the method in this article is correct.

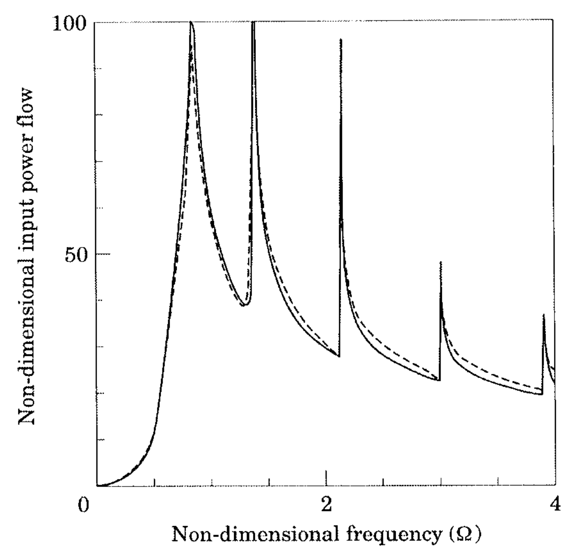

Figure 2. Input power flow into a shell filled-with water for $n = 0$; ——, calculated by the method in [9]; · · · · ·, calculated by this method.

A periodically stiffened cylindrical fluid-filled shell was considered; the following parameters of the coupled system have been used in the calculations, $h = 0{\cdot}02R$, $\mu = 0{\cdot}3$, $\rho = 7850$ kg/m^3, $E = 2{\cdot}07 \times 10^{11}$ N/m^2 and the density of the contained fluid $\rho_0 = 1000$ kg/m^3. The stiffener has a rectangular cross-section (width $b = 0{\cdot}04R$ and height $d = 0{\cdot}04R$). The spacing between adjacent stiffeners is $L = 0{\cdot}4R$. The material parameters of the stiffener are the same as those of the shell.

5.1. INFLUENCE OF STIFFENERS

Figure 3 shows the non-dimensional input power flow P'_{line} plotted against the non-dimensional driving frequency Ω for this stiffened fluid-filled shell excited by a cosine harmonic circumferential line force of circumferential mode order $n = 5$. In order to investigate the influence of the stiffeners, the results of a shell without stiffeners are also plotted.

In three frequency bands, $0{\cdot}1 < \Omega < 0{\cdot}14$, $0{\cdot}4 < \Omega < 0{\cdot}64$ and $1{\cdot}47 < \Omega < 1{\cdot}6$, the power input into the stiffened shell is much less than that into a shell without stiffeners. These frequency bands are named non-propagating bands. This means that the stiffeners greatly influence the input power flow in these frequency bands. The power flow achieves its maximum at the first lower bounding frequency, the second lower and upper bounding frequency. At the first upper bounding frequency and the third lower bounding frequency, the power flow for the stiffened shell is much less than that for an unstiffened shell.

5.2. INFLUENCE OF STIFFENER SPACING

The results for a shell with stiffeners of different spacing are given in Figure 4.

The spacing between adjacent stiffeners in Figure 4(a) is $L = 0{\cdot}8R$, twice that in the original model. There are five frequency bands in which the power input

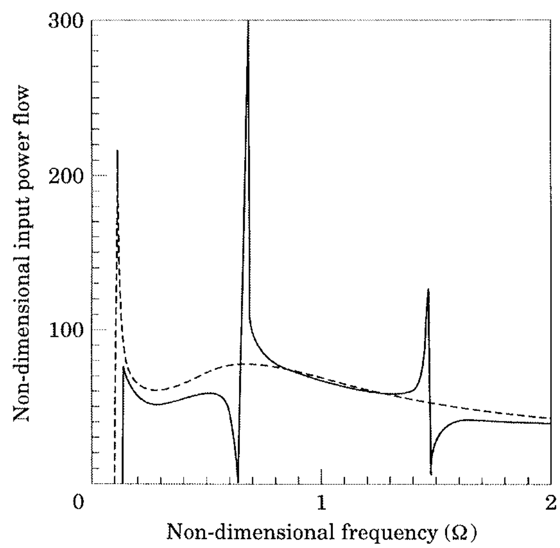

Figure 3. Input power flow into the stiffened shell filled-with water for $n = 5$; ——, stiffened shell; · · · · ·, non-stiffened shell.

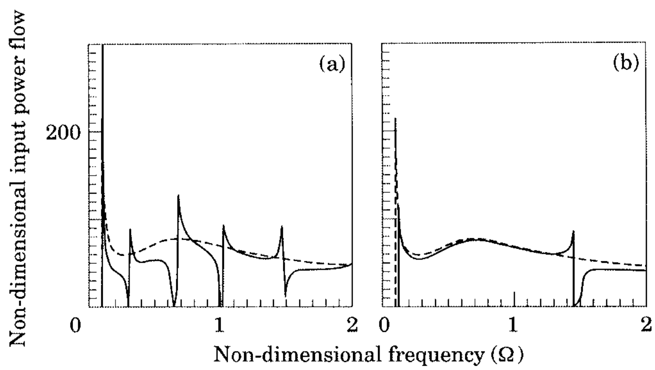

Figure 4. Influence of the stiffener spacing on the input power flow for $n = 5$; ——, stiffened shell; · · · · ·, non-stiffened shell. (a) $L = 0{\cdot}8R$; (b) $L = 0{\cdot}2R$.

into the stiffened shell is much less than that into a shell without stiffeners. When the results of Figure 4(a) are compared with those of Figure 3, it is found that the frequencies of the first, third and fifth non-propagating bands in Figure 4(a) correspond to those of the first, second and third non-propagating bands in Figure 3 respectively. But the bands in Figure 4(a) are narrower than those in Figure 3. The second and fourth non-propagating bands in Figure 4(a) are in the first and second propagating bands in Figure 3.

The stiffener spacing in Figure 4(b) is $L = 0{\cdot}2R$, half of the original model. Only two non-propagating bands exist and the bands are wider than those in Figure 3. It means that once the frequency of the external force is given, the most appropriate stiffener spacing can be chosen to control the input power flow.

5.3. INFLUENCE OF STIFFENER STIFFNESS

The results obtained for modified shell models with stiffeners of different stiffness are plotted in Figure 5. The parameters of the stiffeners in Figure 5(a) are, width $b = 0{\cdot}05R$ and height $d = 0{\cdot}05R$. In Figure 5(b), width $b = 0{\cdot}03R$ and height $d = 0{\cdot}03R$.

When the results of Figure 5(a) are compared with those of Figure 3, it can be found that the input power flow is similar. There are also three non-propagating bands. Each bounding frequency in Figure 5(a) is approximate to the corresponding bounding frequency in Figure 3. The only difference is that the non-propagating bands in Figure 5(a) are wider than those in Figure 3. The results in Figure 5(b) are similar (though the non-propagating bands are narrower) and thus not discussed here. Then, from the point of vibration control, it seems useful to increase the stiffener stiffness.

5.4. INFLUENCE OF CIRCUMFERENTIAL ORDER NUMBER

The results obtained for mode order $n = 1$ and $n = 10$ are shown in Figure 6(a) and Figure 6(b). For mode order $n = 1$, the power flow of the stiffened shell is similar to that of the shell without stiffeners. For mode order $n = 10$, there are also three non-propagating bands. These bands are much wider than those in

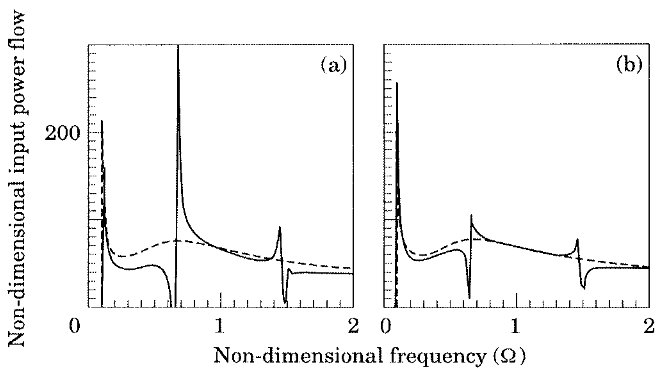

Figure 5. Influence of the stiffener stiffness on the input power flow for $n = 5$; ——, stiffened shell; · · · · ·, non-stiffened shell. (a) $b = d = 0{\cdot}05R$; (b) $b = d = 0{\cdot}03R$.

Figure 3. At each lower bounding frequency, the input power flow achieves its maximum; at each upper bounding frequency, the input power flow equals zero. At the propagating frequency bands, the difference between the results with stiffeners and those without stiffeners is large too. Therefore, it can be concluded that the stiffener can control the input power effectively when the circumferential mode order is high.

6. CONCLUSION

By adopting a periodic structure theory, space-harmonic analysis method, a periodically stiffened cylindrical fluid-filled shell has been investigated. The input power flow from a cosine harmonic circumferential line force of this coupled system has been derived and the results have been obtained for a periodic shell filled with water.

There are propagating bands and non-propagating bands. These bands are greatly influenced by stiffener spacing, stiffener stiffness and the circumferential mode order. Stiffener spacing will influence the number of these bands and the bounding frequencies to a great extent. The non-propagating bands widen with

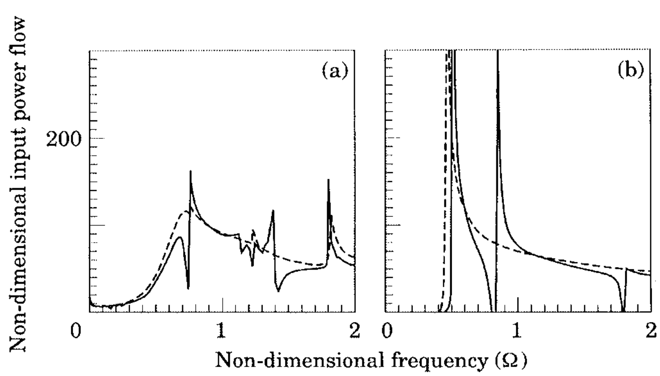

Figure 6. Influence of the circumferential order number on the input power flow; ——, stiffened shell; · · · · ·, non-stiffened shell. (a) $n = 1$; (b) $n = 10$.

an increase in stiffener stiffness. For mode order $n = 1$, the stiffener has little influence on the input power flow. For high mode order, the stiffener can control the input power effectively. From the analysis, one can conclude that once the external load is known, the most appropriate stiffener parameters can be chosen to minimize vibration.

ACKNOWLEDGMENT

The authors are grateful for the financial assistance provided by the National Natural Science Foundation of China (Contract No. 19404005).

REFERENCES

1. Y. K. LIN and T. J. MCDANIEL 1969 *Transactions of the ASME*, *Journal of Engineering for Industry* **91**, 1133–1141. Dynamic of beam-type periodic structures.
2. D. J. MEAD and N. S. BARDELL 1986 *Journal of Sound and Vibration* **111**, 229–250. Free vibration of a thin cylindrical shell with discrete axial stiffeners.
3. D. J. MEAD and N. S. BARDELL 1987 *Journal of Sound and Vibration* **115**, 499–520. Free vibration of a thin cylindrical shell with periodic circumferential stiffeners.
4. W. H. ZHANG and X. M. ZHANG 1991 *Proceedings*, *ASME-PVP*, *Nashville*, *USA*, **214**, 161–166. Vibrational power flow in a cylindrical shell with periodic stiffeners.
5. D. J. MEAD 1970 *Journal of Sound and Vibration* **11**, 181–197. Free wave propagation in periodically supported infinite beams.
6. D. J. MEAD and K. K. PUJARA 1971 *Journal of Sound and Vibration* **14**, 525–541. Space-harmonic analysis of periodically supported beams: response to convected random loading.
7. B. R. MACE 1980 *Journal of Sound and Vibration* **73**, 473–486. Periodically stiffened fluid-loaded plates, I: response to convected harmonic pressure and free wave propagation.
8. B. R. MACE 1980 *Journal of Sound and Vibration* **73**, 487–504. Periodically stiffened fluid-loaded plates, II: response to line and point forces.
9. C. R. FULLER 1983 *Journal of Sound and Vibration* **87**, 409–427. The input mobility of an infinite circular cylindrical elastic shell filled with fluid.
10. M. B. XU and X. M. ZHANG 1998 *Journal of Sound and Vibration* **218**, 587–598. Vibrational power flow in a fluid-filled cylindrical shell.

APPENDIX A: FORCES AND MOMENTS OF A RING STIFFENER

Omitting shear deformation and moment of inertia, the equation of motion of a ring stiffener is

$$\frac{E_1 I}{R_1^4}\left(\frac{\partial^4 w}{\partial\theta^4}-\frac{\partial^3 v}{\partial\theta^3}\right)+\frac{E_1 A}{R_1^2}\left(w+\frac{\partial v}{\partial\theta}\right)+\rho_1 A\frac{\partial^2 w}{\partial t^2}=F_w(\theta,\,t),$$

$$\frac{E_1 I}{R_1^4}\left(\frac{\partial^3 w}{\partial\theta^3}-\frac{\partial^2 v}{\partial\theta^2}\right)+\frac{E_1 A}{R_1^2}\left(\frac{\partial w}{\partial\theta}+\frac{\partial^2 v}{\partial\theta^2}\right)+\rho_1 A\frac{\partial^2 x}{\partial t^2}=F_v(\theta,\,t),$$

$$\frac{E_1 \bar{I}}{R_1^4}\left(\frac{\partial^4 u}{\partial\theta^4}-\frac{\partial^2 (R_1\varphi)}{\partial\theta^2}\right)-\frac{G_1 J}{R_1^4}\left(\frac{\partial^2 u}{\partial\theta^2}+\frac{\partial^2 (R_1\varphi)}{\partial\theta^2}\right)+\rho_1 A\frac{\partial^2 u}{\partial t^2}=F_u(\theta,\,t),$$

$$\frac{E_1\bar{I}}{R_1^2}\left(R_1\varphi-\frac{\partial^2 u}{\partial\theta^2}\right)-\frac{G_1 J}{R_1^2}\left(\frac{\partial^2 u}{\partial\theta^2}-\frac{\partial^2(R_1\varphi)}{\partial\theta^2}\right)+\rho_1 I_p\frac{\partial^2(R_1\varphi)}{\partial t^2}=R_M(\theta,\,t),\quad \text{(A.1)}$$

where $R_1 = R + e_1$; $A = bd$ is the area of stiffener cross-section; I and $\bar{I}$ are moments of gyration; $I_p = I + \bar{I}$ is the polar moment of gyration; J_p is the constant of twist of cross-section; ρ_1 is mass density of stiffener material; E_1 and G_1 are module of elasticity and shear module of stiffener material, respectively; $\varphi = \partial w/\partial x$.

In order to consider the influence of eccentricity, one may express the displacements at the center of the ring in terms of displacement at midsurface

$$u^* = u - e_1\varphi,\qquad v^* = V\left(1+\frac{e_1}{R}\right)-\frac{e_1}{R}\frac{\partial w}{\partial\theta},\qquad w^* = w,\qquad \varphi^* = \varphi,\qquad \text{(A.2)}$$

where e_1 is the distance from the midsurface of shell to the geometric center of stiffener. When $e_1 \ll R$, the second equation is deduced to $v^* = v$.

When the shell vibration is in the nth mode, the ring stiffener vibrations in the same mode, then

$$[u^*\quad v\quad w\quad \varphi]^{\mathrm{T}} = \mathrm{e}^{\mathrm{i}\omega t}[u_a^*\cos n\theta\quad v_a\sin n\theta\quad w_a\cos n\theta\quad \varphi_a\cos n\theta]^{\mathrm{T}},\qquad \text{(A.3a)}$$

$$[F_u\quad F_v\quad F_w\quad M]^{\mathrm{T}} = \mathrm{e}^{\mathrm{i}\omega t}[F_{ua}\cos n\theta\quad F_{va}\sin n\theta\quad F_{wa}\cos n\theta\quad M_a\cos n\theta]^{\mathrm{T}}\quad \text{(A.3b)}$$

From equations (A.1, A.2, A.3) with $\mathrm{e}^{\mathrm{i}\omega t}$ and $\cos n\theta$, $\sin n\theta$ omitted, the forces and moments in the ring stiffener can be expressed as follows:

$$F_w = K_1 w + K_2 v,\qquad F_v = K_2 w + K_3 v,\qquad \text{(A.4a, b)}$$

$$F_u = K_4 u + \left(K_5 - \frac{e_1}{R}K_4\right)\left(R\frac{\partial w}{\partial x}\right),\qquad F_\varphi = RK_5 u + R\left(K_6 - \frac{e_1}{R}K_5\right)\left(R\frac{\partial w}{\partial x}\right),\qquad \text{(A.4c, d)}$$

where

$$K_1 = \frac{R_1}{R}\left(\frac{E_1 I}{R_1^4}n^4 + \frac{E_1 A}{R_1^2} - \rho_1 A\omega^2\right),\qquad K_2 = \frac{R_1}{R}\left(\frac{E_1 I}{R_1^4}n^3 + \frac{E_1 A}{R_1^2}n\right),\quad \text{(A.5a, b)}$$

$$K_3 = \frac{R_1}{R}\left(\frac{E_1 I}{R_1^4}n^2 + \frac{E_1 A}{R_1^2}n^2 - \rho_1 A\omega^2\right),\qquad K_4 = \frac{R_1}{R}\left(\frac{E_1\bar{I}}{R_1^4}n^4 + \frac{G_1 J}{R_1^4}n^2 - \rho_1 A\omega^2\right),\qquad \text{(A.5c, d)}$$

$$K_5 = \frac{1}{R}\left(\frac{E_1\bar{I}}{R_1^2}n^2 + \frac{G_1 J}{R_1^2}n^2\right),\qquad K_6 = \frac{1}{R}\left(\frac{E_1\bar{I}}{R_1^2} + \frac{G_1 J}{R_1^2}n^2 - \rho_1\omega^2 I_p\right).\qquad \text{(A.5e, f)}$$

APPENDIX B: LIST OF SYMBOLS

A	area of stiffener cross-section
b	stiffener width
c_0	sound velocity in the contained fluid
d	stiffener height
D	membrane stiffness
E, E_1	Young's modulus of shell material or stiffener material
e_1	distance from midsurface of shell to geometric of stiffener
F	applied line force
f_u, f_v, f_w	external loads exerted on the shell
F_u, F_v, F_w, M	forces or moment in the stiffener
FL	fluid loading term
G_1	shear modulus of stiffener material
h	shell wall thickness
i	$\sqrt{-1}$
I, $\bar{I}$	moments of gyration of stiffener cross-section
$I_p = I + \bar{I}$	polar moment of gyration of stiffener cross-section
J_p	constant of twist of stiffener cross-section
J_n	Bessel function of order n
k_0	free wavenumber
k_x	axial wavenumber
k_s^r	radial wavenumber
L	stiffener spacing
n	circumferential modal number
p	applied harmonic pressure
P_{point}	input power from a point force
P_{line}	input power from a line force
P'_{line}	non-dimensional input power from a line force
R	shell mean radius
$R_1 = R + e_1$	radius of geometric center of stiffener
u, v, w, $\partial w/\partial x$	shell displacements
x, θ, r	cylindrical co-ordinate
ρ_0, ρ, ρ_1	density of fluid, shell material or stiffener material
η	loss factor
μ	Poisson's ratio
ω	circular frequency
Ω	non-dimension frequency
λ	non-dimension wavenumber
δ	Dirac delta function

Superscripts

$\otimes$	complex conjugate
$'$	differentiation